# Electron spin resonance above $T_C$ in layered manganites

N. O. Moreno, P. G. Pagliuso, and C. Rettori
*Instituto de Física ''Gleb Wataghin,'' UNICAMP, 13083-970, Campinas-SP, Brazil*

J. S. Gardner, J. L. Sarrao, and J. D. Thompson
*Los Alamos National Laboratories, Los Alamos, New Mexico 87545*

D. L. Huber
*University of Wisconsin-Madison, Madison, Wisconsin 53706*

J. F. Mitchell
*Argonne National Laboratory, Argonne, Illinois 60439-4845*

J. J. Martinez and S. B. Oseroff
*San Diego State University, San Diego, California 92182*
(Received 23 October 2000; published 5 April 2001)

We have performed electron spin resonance (ESR) and dc magnetization measurements on single crystals of $La_{2(1-x)}Sr_{1+2x}Mn_2O_7$ up to 800 K with special emphasis on the $x=0.4$ composition. The ESR linewidth shows behavior similar to that observed in the three-dimensional perovskites and above ~500 K can be described by a universal expression $\Delta H_{pp}(T)=[C/T\chi(T)]\Delta H_{pp}(\infty)$. The linewidth and the resonance field become anisotropic below ~500 K. The anisotropy in the resonance field is proportional to the magnetization $M$, and we concluded that it is intrinsic to the system. We show that demagnetization effects can explain only part of the anisotropy. The remainder arises from short-range uniaxial terms in the Hamiltonian that are associated with the crystal field and Dzialozhinsky-Moriya interactions. The anisotropy in the linewidth is attributed to the easy-plane ferromagnetic ordering, which also arises from the short-range anisotropy.

DOI: 10.1103/PhysRevB.63.174413 PACS number(s): 78.30.−j, 75.30.−m, 63.20.−e, 72.10.Di

## I. INTRODUCTION

The observation of colossal magnetoresistance (CMR) in the series of Ruddlesden-Popper (RP) phases,[1] $A_{n+1}Mn_nO_{3n+1}$, has attracted considerable attention. Most of the work was done in the perovskite manganite $La_{1-x}Sr_x(Ca)MnO_3$ ($n=\infty$). Recently, the $n=2$ member $A_3Mn_2O_7$ has received considerable attention due to its interesting properties. The RP phases consist of $n$ layers of perovskite octahedra blocks along the $c$ axis. The blocks are separated by the insertion of rocksalt layers of $A_2O_2$, which leads to a larger $c$-axis lattice parameter. Moritomo *et al.*[2] observed CMR in the layered $La_{1.2}Sr_{1.8}Mn_2O_7$ at $T_C$ ~125 K, which nominally corresponds to 40% of the hole doping. Lately, our group and others have studied by electron spin resonance (ESR) the $T$ dependence of the ESR linewidth, $\Delta H_{pp}$, for three-dimensional (3D) perovskites and pyrochlores.[3–6] By measuring ESR and dc susceptibility up to high $T$, $T \gtrsim 3T_C$, we found that $\Delta H_{pp}$ in the paramagnetic region, for the 3D perovskites and pyrochlores, presents a universal behavior that can be described by the expression

$$\Delta H_{pp}(T)=[C/T\chi(T)]\Delta H_{pp}(\infty), \tag{1}$$

where $\chi(T)$ is the dc susceptibility and $\Delta H_{pp}(\infty)$ is the high-$T$ limit of the linewidth associated with the parameters of the Hamiltonian describing the interactions of the spin system.[3–5] From these data the role played in the linewidth by interactions such as the magnetic anisotropy, superexchange, and double exchange can be extracted. For this reason, we felt that it was interesting to perform a similar study on the layered manganites. We tried also to clarify some discrepancies in the interpretation of the data reported in the literature about an increase of the magnetization $M$ observed at ~300 K in $(La,Sr)_3Mn_2O_7$, claimed to be intrinsic to the layer systems by some authors and extrinsic by others.[7] For example, Potter *et al.* concluded that the high-$T$ transition was not intrinsic to the $n=2$ system, and was associated with intergrowths of other RP phases.[8] Instead, Chauvet *et al.*, who reported ESR on layered $La_{1.35}Sr_{1.65}Mn_2O_7$ powders, observed at ~350 K, well above $T_C$ ~110 K, that the ESR spectrum splits into two lines and concluded that both lines were intrinsic to the system.[9]

In this work we report measurements as a function of angle, frequency, and magnetic field of the ESR and $M$ in several single crystals of $La_{1.2}Sr_{1.8}Mn_2O_7$ up to 800 K. We have also studied a single crystal and a powder of $La_{1.35}Sr_{1.65}Mn_2O_7$ and for completeness made some measurements on single crystals with $0.33 \lesssim x \lesssim 0.38$.

## II. EXPERIMENTAL TECHNIQUES

We have carried out systematic ESR and dc magnetization measurements on several single crystals of $La_{1.2}Sr_{1.8}Mn_2O_7$ of $\sim 1\times 1\times 0.1$ mm$^3$ and in powder and a crystal of $La_{1.35}Sr_{1.65}Mn_2O_7$. In order to prepare the crystals, polycrystalline materials were synthesized by a solid-state reaction of stoichiometric quantities of $MnO_2$, $SrCO_3$, and $La_2O_3$ at temperatures up to 1550 °C in air. Polycrystalline

 

material was shown from x-ray diffraction to be free of other members of the Ruddlesden-Popper series ($\lesssim 3\%$ by volume). The polycrystalline compounds were then used as starting materials for the crystal growth. Crystals were melt grown in a flow of $O_2$ using a floating zone optical image furnace. We found that the amount of impurity phases increased when the growth rate was increased. Nonetheless, there is a point where the losses became too great when the growth process was slowed down and a gradient in the crystals composition is observed. It is also true that two identical growths do not produce the same amount of impurities, although there are general trends (slower is better, at least over small distances). Ideal growth conditions for controlling the extrinsic phases were not found. However, we obtained a set of parameters which produced single crystals with a very low volume fraction of extrinsic phases. The resulting boule contained many shiny black platelike crystals with the crystallographic *c* axis perpendicular to the plate. The crystals could easily be cleaved away. In this study we examine several crystals. The crystal known here as sample $S_1$ has the lower impurity phase content and was grown at a rate of 4 mm/h. The ESR experiments were carried out in a Bruker ESR spectrometer at 9.5 GHz in the range of temperature between 100 K and 700 K and at 35 GHz between 100 K and 300 K. The *M* data were taken in a MPMS-5 Quantum Design superconducting quantum interference device (SQUID) magnetometer between 2 K and 800 K.

### III. RESULTS AND DISCUSSION

All the samples were characterized by measuring their dc susceptibility and *M* up to 800 K. From the high-*T* susceptibility we obtained the number of Bohr magnetons, $4.77(5)\mu_B$, and $4.7(1)\mu_B$, close to the expected ones, $4.49\mu_B$ and $4.57\mu_B$, and values of the Curie-Weiss temperature, $\Theta_{CW}=280(5)$ K and 270(5) K, for $La_{1.2}Sr_{1.8}Mn_2O_7$ and $La_{1.35}Sr_{1.65}Mn_2O_7$, respectively. Ordering temperatures of $T_C \sim 125$ K and $\sim 112$ K and saturation magnetic moments, below $T_C$, of $\sim 3.6(1)\mu_B$/Mn were obtained for $La_{1.2}Sr_{1.8}Mn_2O_7$ and $La_{1.35}Sr_{1.65}Mn_2O_7$, in agreement with previous reports.[10]

In the paramagnetic regime, a Dysonian resonance line with $g=2.0$ is measured for 500 K$\lesssim T \lesssim$800 K for all the crystals studied. Its intensity *I* follows reasonably well the *T* dependence of $\chi_{dc}(T)$, as observed in the perovskites and pyrochlore manganites.[3,5] Below $\sim 500$ K a shift of the resonance field $H_r^{ESR}$ is measured. The shift depends on the direction of the external magnetic field *H* with respect to the crystallographic axes of the sample. We found that within the experimental error, the shift is the same for three different crystals of $La_{1.2}Sr_{1.8}Mn_2O_7$, labeled as $S_1$, $S_2$, and $S_3$. In Fig. 1 the shift from $g=2.0$, $H_r^{ESR}-H_{g=2}$ vs *T*, is given for the three samples, with $H\|[a,b]$ plane and $H\|c$ axis at $\sim 9.5$ GHz. The shift of a powder obtained from sample $S_3$ is also included in Fig. 1. The inset shows the angular dependence between the *c* axis and the $[a,b]$ plane of $H_r^{ESR}$ at $T=230$ K. In Fig. 2 the shift $H_r^{ESR}-H_{g=2}$ vs *M*, with $H\|[a,b]$ plane and $H\|c$ axis, is given for $S_1$ and $S_2$ for $T \gtrsim T_C$. As can be seen the shift of $H_r^{ESR}$ scales linearly with *M*. The *M* given in Fig. 2 was measured at $H=H_r^{ESR}$. As *T* approaches $T_C$ the ESR line intensity grows dramatically, and its anisotropy rapidly increases. For $T<T_C$ the angular variation of this resonance can be measured. The linewidth gets broader as *T* approaches $T_C$, but does not get distorted as occurs for the 3D perovskite systems. The *T* dependence of $\Delta H_{pp}(T)$ is given in Fig. 3, together with the fitting of $\Delta H_{pp}(T)$ to Eq. (1). Above $\sim 450$ K, $\Delta H_{pp}$ is isotropic and is described reasonably well by Eq. (1) with $\Delta H_{pp}(\infty)=1.7(1)$ kOe. For $T\lesssim 450$–$500$ K a departure of $\Delta H_{pp}(T)$ from Eq. (1) is observed (see Fig. 3). A behavior similar to the one described above was observed for ESR measured in a single crystal of $La_{1.35}Sr_{1.65}Mn_2O_7$. We have also measured ESR, but not in such detail, on single crystals with different compositions, $0.33\lesssim x\lesssim 0.38$. In all of these cases we found a similar dependence of the ESR linewidth and

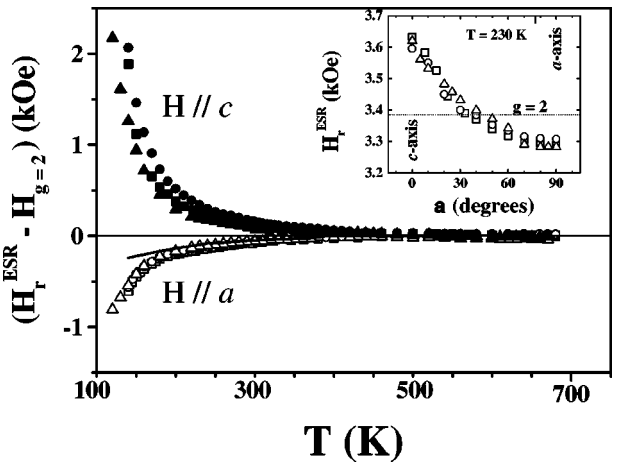


FIG. 1. *T* dependence of the resonance shift, $H_r^{ESR}-H_{g=2}$, for $H\|a$ axis (open symbols) and $H\|c$ axis (solid symbols), for the $S_1$ (□), $S_2$ (○), and $S_3$ (△) crystals and powder of $S_3$ (−). The inset shows the ESR angular variation of $H_r^{ESR}$ for $S_1$, $S_2$, and $S_3$ at 230 K [$H\|c$ ($\alpha=0°$) and $H\|a$ ($\alpha=90°$)].

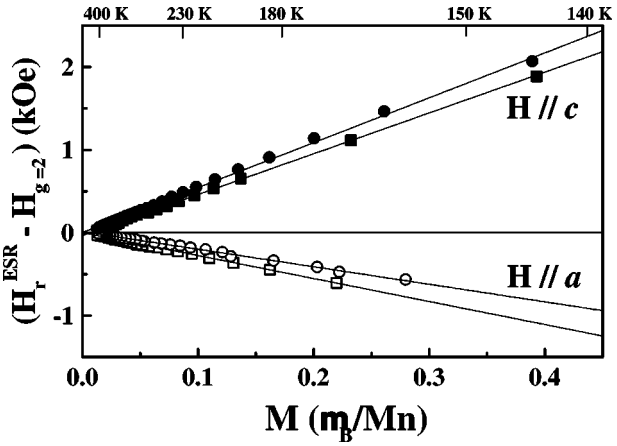


FIG. 2. *M*-linear dependence of the resonance shift, $H_r^{ESR}-H_{g=2}$, for $H\|a$ axis (open symbols) and $H\|c$ axis (solid symbols), for the $S_1$ (□) and $S_2$ (○) crystals.

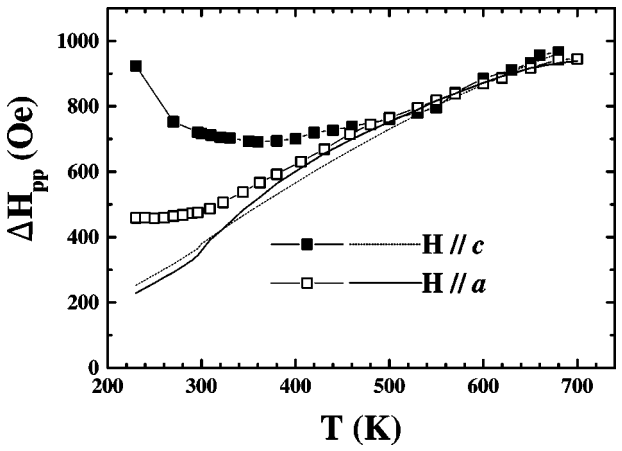


FIG. 3. The peak-to-peak ESR linewidth $\Delta H_{pp}$ for the $S_1$ crystal as a function of $T$ measured at 9.4 GHz. Dashed and solid lines are the fittings using Eq. (1) for $H\|c$ axis and $H\|a$ axis, respectively.

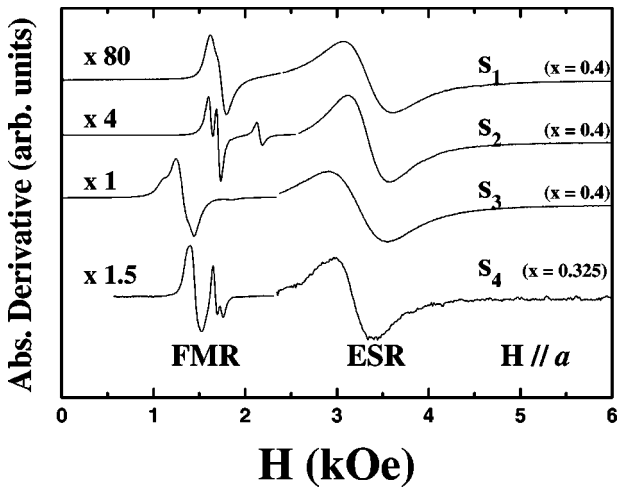


FIG. 4. ESR spectra at 230 K for the $S_1$, $S_2$, $S_3$, and $S_4$ crystals with $H\|a$ axis. Notice the much higher $I$ of the FMR for $S_3$ and $S_4$ relative to that of $S_1$ and $S_2$.

resonance field as a function of $T$ and microwave frequency (magnetic field) as observed for $x=0.40$ and $x=0.325$.

As other authors, we observed an increase of $M$ for $T \sim 300$ K$\gg T_C$ for all the samples studied.[7–9] We obtained the volume of the sample required to account for that increase of $M$ above $T_C$, as done previously by Potter *et al.*[8] We estimated it from the number of Bohr magnetons obtained from the hysteresis loops normalized by the saturation magnetic moment measured at high field. We found that the volume of the sample required us to explain why the step on $M$ at the temperature where it appears was different even for samples with the same value of $x$. The volumes calculated for the three single crystals studied for $La_{1.2}Sr_{1.8}Mn_2O_7$, labeled $S_1$, $S_2$, and $S_3$, were $\lesssim 0.03\%$, $\sim 0.25\%$, and $\sim 1\%$, respectively, and $\sim 0.6\%$ for the single crystal $S_4$ of $La_{1.35}Sr_{1.65}Mn_2O_7$. Thus, the sudden increase of $M$ observed at $T \approx 300$ K is sample dependant; i.e., the increase in $M$ is due to the presence of extrinsic phases as previously concluded by Potter *et al.* Further support for this conclusion is that we observed the appearance of new resonance lines [ferromagnetic resonance (FMR)] for all the samples studied at $T$ close to where the step in $M$ is first seen. For the $H\|[a,b]$ plane the FMR lines shift to lower fields as $T$ decreases. Figure 4 shows the spectra with $H\|a$ axis at 230 K for the single crystals $S_1$, $S_2$, and $S_3$, of $La_{1.2}Sr_{1.8}Mn_2O_7$ and $S_4$ of $La_{1.35}Sr_{1.65}Mn_2O_7$. As seen in Fig. 4 the main difference is that the intensities $I$ of the FMR lines are larger for the samples with larger impurity content. For all the samples, the increase in $I$ of the FMR corresponds to the increase of $M$ observed at a similar $T$. Thus, the step on $M$ found well above $T_C$ is associated with the appearance of the FMR lines. The volume fraction required, for all the samples studied, to explain the extra $M$ observed at high $T$ and the $I$ of the FMR are the same within experimental error, once corrected for skin depth effects. The features described above are possibly due to small regions which order ferromagnetically in the samples and are not intrinsic as previously claimed.[9] For comparison we prepared a powder of $La_{1.35}Sr_{1.65}Mn_2O_7$; the powder was obtained from the original single crystal $S_4$. As Chauvet *et al.*, we observed the appearance of an extra FMR broad line below $\sim 350$ K, instead of several narrow lines as seen in Fig. 4 for the single crystal $S_4$ of $La_{1.35}Sr_{1.65}Mn_2O_7$. That is possibly due to the high anisotropy of the FMR lines associated with the extrinsic phases. Recently, Bhagat *et al.*[11] had observed a similar ESR spectrum below 300 K in a sample of $La_{1.2}Sr_{1.8}Mn_2O_7$ with a content of extrinsic phases similar to our $S_3$ sample and also came to the conclusion that the extra FMR lines are due to impurity phases.

In general, for paramagnetic materials demagnetizing effects can be neglected as the $M$ is small. But for these concentrated systems, with applied fields of $H \sim 3$–$4$ kOe (9.5 GHz) and $\sim 11$–$13$ kOe (35 GHz), a shift of several hundred Oe is expected for $H\|[a,b]$ plane and $H\|c$ axis for $T \lesssim 200$ K. Thus, the internal field $H_i$ within the sample must be corrected for the demagnetizing field. For it, the demagnetizing tensor $N$, which depends on the shape of the sample, needs to be known. The principal values determining the angular variations of the resonance field can be exactly calculated only for simple cases: infinite plate, disk, etc.[12–14] Our samples may be approximated by an infinite plate. The shift measured, shown in Figs. 1 and 2, has the dependence expected, $\omega/\gamma = H_r^{ESR} - 4\pi M$ and $\omega/\gamma = [H_r^{ESR}(H_r^{ESR} + 4\pi M)]^{1/2}$, for $H\|c$ axis and $H\|[a,b]$ plane, respectively. That is not surprising as $H_r^{ESR}$ is much larger than $4\pi M$. We found that the shift $H_r^{ESR} - H_{g=2}$ scales with the frequency measured, 9 GHz and 35 GHz. Thus, it seems reasonable to conclude that the line shift is intrinsic to $n=2$ compounds as it is similar to all the samples measured. In spite of the good qualitative agreement, the observed $g$ shift is about 3 times larger than predicted from demagnetizing fields. Thus, the mechanism responsible for the observed shift is not fully explained by demagnetizing effects alone. It should be noted that similar shifts have been observed before.[15,16] In the case of low-dimensional organic radical magnets, the shift was first attributed to short-range magnetic order. Recently, however, the importance of demagnetizing fields over short-range order has been emphasized in order to explain the resonance fields in these compounds.[17] In the layered

manganites, the $g$ factors are not only anisotropic but also strongly $T$ dependent, varying rapidly near $T_C$. The *qualitative* behavior of the $g$ factors resembles the behavior associated with the demagnetizing effects; as noted, however, the *magnitude* of the variation in $g_a$ and $g_c$ is about a factor of 3 larger than one would expect from the measured values of $4\pi M$. We return to this point below. As mentioned above for $La_{1.2}Sr_{1.8}Mn_2O_7$ and $La_{1.35}Sr_{1.65}Mn_2O_7$ in spite of the broadening of the ESR linewidth at $T\sim T_C$ the line is almost undistorted and the expected anisotropy for a FM plate is observed. For $T\lesssim T_C$, the anisotropy of the FMR can be accounted for by a magnetization $M$, corresponding to the full moment obtained for the Mn ion, $3.6(1)\mu_B$/Mn.

Since the demagnetizing effects account for no more than about one-third of the $g$-factor variation, one must look to other mechanisms. As noted elsewhere,[4] in manganite systems, the anisotropy is dominated by contributions from the crystal field (single-ion) and the Dzialozhinsky-Moriya (antisymmetric exchange) interactions. Both of these interactions are far stronger than the dipolar coupling as evidenced by the fact that the ESR linewidth is $\sim 10^3$ times larger than the width expected from the dipolar mechanism alone. We argue that the short-range anisotropic interactions are also largely responsible for the $g$-factor variation. To see how this can happen, we consider the effect of a single-ion anisotropy term of the form

$$\sum_j (A_x S_{xj}^2 + A_y S_{yj}^2 + A_z S_{zj}^2), \tag{2}$$

where $x,y,z$, refer to the crystallographic axes, which are assumed to coincide with the ellipsoidal axes of the sample. We follow Van Vleck's[18] microscopic derivation of Kittel's formula for the ferromagnetic resonance frequency.[19] In the analysis, we take the static field from the $z$ direction, and we consider the equations of motion for the $x$ and $y$ components of the total spin, $S_x=\Sigma_j S_{xj}$ and $S_y=\Sigma_j S_{yj}$. In the presence of the dipolar interaction and the crystal field anisotropy, the equations of motion for $S_x$ and $S_y$ become

$$\frac{dS_x}{dt} = -2\mu_B H S_y + (N_z - N_y) 2\mu_B M S_y + \Sigma_j (A_y - A_z)(S_{yj}S_{zj} + S_{zj}S_{yj}), \tag{3}$$

$$\frac{dS_y}{dt} = +2\mu_B H S_x - (N_z - N_x) 2\mu_B M S_x - \Sigma_j (A_x - A_z)(S_{xj}S_{zj} + S_{zj}S_{xj}), \tag{4}$$

where $M$ is the magnetization and the $N_i$ denote the demagnetizing factors. Since $S>1/2$, we can linearize these equations by substituting for $S_{zj}$ its thermal average $\langle S_z\rangle$, which we take to be the same for all spins. Following linearization, we replace $\langle S_z\rangle$ by $M/(-2\mu_B\rho_S)$, where $\rho_S$ is the number of spins per unit volume. After taking these steps we obtain

$$\frac{dS_x}{dt} = -2\mu_B H S_y + \left[ N_z + \frac{A_z}{2\mu_B^2\rho_S} - N_y - \frac{A_y}{2\mu_B^2\rho_S} \right] 2\mu_B M S_y, \tag{5}$$

$$\frac{dS_y}{dt} = +2\mu_B H S_x - \left[ N_z + \frac{A_z}{2\mu_B^2\rho_S} - N_x - \frac{A_x}{2\mu_B^2\rho_S} \right] 2\mu_B M S_x. \tag{6}$$

From these equations, it is evident that the effect of the anisotropy is to modify the demagnetization factors according to the equation $N_i \to N_i + A_i/(2\mu_B^2\rho_S)$. The added terms are on the order of the ratio of the (nondipolar) anisotropy energy to the dipolar energy. Since the ESR linewidth is approximately the ratio of the square of the anisotropy (or dipolar) field to the exchange field, a very crude estimate of $A_i/(2\mu_B^2\rho_S)$ is given by the ratio of the square root of the high-$T$ limit of the ESR linewidth to the square root of the width expected from dipolar interactions only; in other words, we have $A_i/(2\mu_B^2\rho_S)\approx 10$–$100$. Because the bilayer materials are easy-plane ferromagnets for $x>0.32$, we have $A_x=A_y=A_\perp$ and $A_z=A_\parallel>A_\perp$, when the $z$ direction coincides with the crystallographic $c$ (hard) axis.[10]

Although the above analysis was carried out for a very simple model of the anisotropy—single ion, all sites equivalent—we expect the qualitative features of the results to be preserved in a more realistic calculation. After linearization, the equations of motion will contain terms of the form $\Sigma_j C_j\langle S_{zj}\rangle$ ($S_{xj}$ or $S_{yj}$). Although these terms cannot be brought to the form $C\langle S_z\rangle$ ($S_{xj}$ or $S_{yj}$) without further approximations, we expect their contribution to the $g$ factors to be similar to that found previously for the single-ion mechanism. For an easy-plane system, with the field along the $c$ axis, one predicts that $\omega/\gamma=[H_r^{ESR}-(N_\parallel-N_\perp)M - f(T,H_r^{ESR})]$, whereas when the field is perpendicular to the $c$ axis, one has $\omega/\gamma=\{H_r^{ESR}[H_r^{ESR}+(N_\parallel-N_\perp)M + f(T,H_r^{ESR})]\}^{1/2}$. The function $f(T,H)$ depends on the details of the anisotropy mechanism but is proportional to $H$ for small fields and is expected to increase in magnitude as $T\to T_C$. Although second-order anisotropy enters into the equation for $\omega$ in a matter similar to the demagnetizing corrections, the short-range anisotropy term does not depend on the shape of the sample.

According to the theory outlined in Ref. 16, in uniaxial systems the ESR linewidth (in frequency units) with the static field along the $c$ axis is equal to the zero-field relaxation rate for spin fluctuations along the $a$ axis, whereas when the static field is along the $a$ axis, the ESR linewidth is equal to the average of the zero-field relaxation rates along the $a$ and $c$ axes. That is to say, we have

$$(\mu_B/h) g_c \Delta H_c = \frac{1}{\mathcal{T}_{2a}} \tag{7}$$

and

$$(\mu_B/h) g_a \Delta H_a = \frac{1}{2}\left( \frac{1}{\mathcal{T}_{2a}} + \frac{1}{\mathcal{T}_{2c}} \right). \tag{8}$$

The $T$ dependences we find for $g_c\Delta H_c$ and $g_a\Delta H_a$ are compatible with a slow variation in $1/\mathcal{T}_{2c}$ and a divergence in $1/\mathcal{T}_{2a}$ in the limit of $T\to T_C$. Since the bilayer compound is an easy-plane ferromagnet, it is expected that the critical

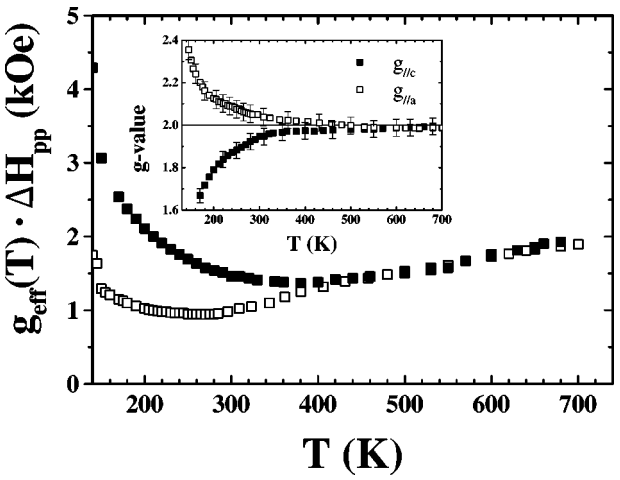


FIG. 5. $T$ dependence of the product $g_{eff}\Delta H_{pp}$ for $S_1$, $H\|c$ (■), $H\|a$ (□). The inset shows the $T$ dependence of the $g$ factor for the same sample for $H\|c$ axis (■) and $H\|a$ axis (□).

behavior would be most pronounced for fluctuations in the plane perpendicular to the $c$ axis. With divergent behavior only in $1/\mathcal{T}_{2a}$, both $g_a\Delta H_a$ and $g_c\Delta H_c$ will increase and the ratio of $g_c\Delta H_c$ to $g_a\Delta H_a$ will approach 2 as $T\rightarrow T_C$. It is evident from Fig. 5 that this happens for 400 K$>T>$170 K. For $T<170$ K, the ratio of the linewidths is significantly greater than 2, which may indicate that close to $T_C$, critical effects are suppressed when the applied field is in the easy plane. It would be interesting to take similar data by making minor scratches in a high-quality single crystal of $La_{1.4}Sr_{1.6}Mn_2O_7$, $x=0.3$, where the easy axis lies along the $c$ axis instead of the $[a,b]$ plane for $x\gtrsim 0.32$.[10]

## IV. CONCLUSIONS

In the paramagnetic region, above ~450 K, the ESR linewidth can be fitted reasonably well by Eq. (1) with $\Delta H_{pp}(\infty)=1.7(1)$ kOe. At this point, a comparison with other bilayers manganites compounds is not possible, due to the lack of data. However, we can attempt to compare it with other 3D perovskites with similar values of $\Theta_{CW}$; we concluded then that the double-exchange mechanism does not seem to play an important role in the exchange narrowing of the ESR line, as is also the case for the 3D perovskites.[4] We measured a shift of the resonance field for the intrinsic ESR line of the layer compound for $T\sim 450$–$500$ K$\gg T_C$. We found that the shift is independent of the impurity phase content and could be accounted for only partially by demagnetizing effects. Other contributions to the shift come from the short-range uniaxial terms in the Hamiltonian that are associated with the crystal field and Dzialozhinsky-Moriya interactions, although the latter are expected to be small (see the Appendix). Also, it might be argued that the extrinsic phases give rise to regions of spins with enhanced susceptibility that may magnify the effect of the demagnetizing fields. However, the fact that similar results were obtained for samples with a wide distribution of extrinsic phases does not seem to support that argument. These results may be important when measuring in a magnetic field for $T\gtrsim T_C$; i.e., some of the changes in the spectra observed above $T_C$ could be associated with demagnetizing fields. We have also observed an anisotropy in the $\Delta H_{pp}$ below 500 K which appears to be connected with the easy-plane character to the ordering at $T_C$. Finally, we have confirmed that the sudden increase in $M$ well above $T_C$ is due to impurity phases.

## ACKNOWLEDGMENTS

This work was supported by FAPESP Grant Nos. 95/4721-4, 97/03065-1, 97/11563-1 São Paulo-SP-Brazil, CAPES-Brazil, NSF-INT Grant No. 9602829, and NSF-DMR Grant No. 9705155. Work done at Los Alamos was conducted under the auspices of the U.S. DOE. J.S.G. thanks Dr. K. McClellan and J.M. Roper for assistance with the crystal growths.

## APPENDIX

A simple calculation suggests that the contribution to the shift in the $g$ factor coming from the Dzialozhinsky-Moriya (DM) interaction may be quite small. Consider a pair of spins coupled by both the Heisenberg exchange interaction and the DM interaction, $\mathbf{D}_{12}\cdot(\mathbf{S}_1\times\mathbf{S}_2)$, with the static field along the $z$ axis. After linearization, the equation of motion for the $x$ component of the the total spin, $S_{x1}+S_{x2}$, has the form

$$\frac{d(S_{x1}+S_{x2})}{dt}=-2\mu_B H(S_{y1}+S_{y2})+D_{12}^z\langle S_z\rangle(S_{x1}-S_{x2}), \tag{A1}$$

with a similar equation for $S_{y1}+S_{y2}$. Note that because of the antisymmetric nature of the DM term, the transverse components of the total spin, $\mathbf{S}_1+\mathbf{S}_2$, couple to the transverse components of the difference spin, $\mathbf{S}_1-\mathbf{S}_2$. Unlike the total spin, the difference spin does not commute with the Heisenberg Hamiltonian. As a consequence, the term on the right hand side of Eq. (A1) fluctuates rapidly over the time scale of the Larmor period, and thus does not contribute significantly to the $g$ factor. This is in contrast to single-ion anisotropy which does couple with the transverse components of the total spin [see Eq. (5)].

[1] S.N. Ruddlesden and P. Popper, Acta Crystallogr. **11**, 54 (1958).
[2] Y. Moritomo, A. Asamitsu, H. Kuwahara, and Y. Tokura, Nature (London) **380**, 141 (1996).
[3] M.T. Causa, M. Tovar, A. Caneiro, F. Prado, G. Ibanez, C.A. Ramos, A. Butera, B. Alascio, X. Obradors, S. Pinol, F. Rivadulla, C. Vazquez, A. Lopez-Quintela, J. Rivas, Y. Tokura, and S.B. Oseroff, Phys. Rev. B **58**, 3233 (1998); M.T. Causa, G. Alejandro, M. Tovar, P.G. Pagliuso, C. Rettori, S.B. Oseroff, and M.A. Subramanian, J. Appl. Phys. **85**, 5408 (1999).
[4] D.L. Huber, G. Alejandro, A. Caneiro, M.T. Causa, F. Prado, M.

Tovar, and S.B. Oseroff, Phys. Rev. B **60**, 12 155 (1999).
[5] S.B. Oseroff, N.O. Moreno, P.G. Pagliuso, C. Rettori, D.L. Huber, J.S. Gardner, J.L. Sarrao, J.D. Thompson, M.T. Causa, F. Prado, M. Tovar, and B.R. Alascio, J. Appl. Phys. **87**, 5810 (2000).
[6] M.S. Seehra, M.M. Ibrahim, V.S. Babu, and G. Srinivasan, J. Phys.: Condens. Matter **8**, 11 283 (1996); M. Dominguez, S.E. Lofland, S.M. Bhagat, A.K. Raychaudhuri, H.L. Ju, T. Venkates, and R.L. Greene, Solid State Commun. **97**, 193 (1996); S.E. Lofland, P. Kim, P. Dahiroc, S.M. Bhagat, S.D. Tyagi, S.G. Karabashev, D.A. Shultyatev, A.A. Arsenov, and Y. Mukovskii, Phys. Lett. A **233**, 476 (1997).
[7] T. Kimura, Y. Tomioka, H. Kuwahara, A. Asamitsu, M. Tamura, and Y. Tokura, Science **274**, 1698 (1996); T.G. Perring, G. Aeppli, Y. Moritomo, and Y. Tokura, Phys. Rev. Lett. **78**, 3197 (1997); J.-S. Zhou, J.B. Goodenough, and J.F. Mitchell, Phys. Rev. B **58**, 579 (1998); J.-S. Zhou and J.B. Goodenough, Phys. Rev. Lett. **80**, 2665 (1998); T.M. Kelley, D.N. Argyriou, R.A. Robinson, H. Nakotte, J.F. Mitchell, R. Osbron, and J.D. Jorgensen, Physica B **241-243**, 439 (1998); R.H. Heffner, D.E. MacLaughlin, G.J. Nieuwenhuys, T. Kimura, G.M. Luke, Y. Tokura, and Y.J. Uemura, Phys. Rev. Lett. **81**, 1706 (1998).
[8] C.D. Potter, M. Swiatek, S.D. Bader, D.N. Argyriou, J.F. Mitchell, D.J. Miller, D.G. Hinks, and J.D. Jorgensen, Phys. Rev. B **57**, 72 (1998).
[9] O. Chauvet, G. Goglio, P. Molinie, B. Corraze, and L. Brohan, Phys. Rev. Lett. **81**, 1102 (1998).
[10] K. Hirota, Y. Moritomo, H. Fujioka, M. Kubota, H. Yoshizawa, and Y. Endoh, J. Phys. Soc. Jpn. **67**, 3380 (1998); J.Q. Li, Y. Matsui, T. Kimura, and Y. Tokura, Phys. Rev. B **57**, R3205 (1998); T. Kimura, R. Kumai, Y. Tokura, J.Q. Li, and Y. Matsui, *ibid.* **58**, 11 081 (1998); T. Hayashi, N. Miura, M. Tokunaga, T. Kimura, and Y. Tokura, J. Phys.: Condens. Matter **10**, 11 525 (1998); R. Suryanarayanan, G. Dhalenne, A. Revcolevschi, W. Prellier, J.P. Renard, C. Dupas, W. Caliebe, and T. Chatterji, Solid State Commun. **113**, 267 (2000); M. Kubota, H. Fujioka, K. Ohoyama, K. Hirota, Y. Moritomo, H. Yoshizawa, and Y. Endoh, J. Phys. Chem. Solids **60**, 116 (1999).
[11] S.M. Bhagat, S.E. Lofland, and J.F. Mitchell, Phys. Lett. A **259**, 326 (1999).
[12] C. Kittel, *Introduction to Solid State Physics* (Wiley, New York 1997).
[13] M. Okochi, J. Phys. Soc. Jpn. **28**, 897 (1970).
[14] C. Victoria, R.C. Barker, and A. Yelon, Phys. Rev. Lett. **19**, 792 (1967).
[15] K. Nagata, J. Phys. Soc. Jpn. **40**, 1209 (1976); see also K. Nagata, I. Yamamoto, H. Takano, and Y. Yokozawa, *ibid.* **43**, 857 (1977) and references therein.
[16] D.L. Huber and M.S. Seehra, Phys. Status Solidi B **74**, 145 (1976).
[17] J.-L. Stanger, J.-J. Andre, P. Turek, Y. Hosokoshi, M. Tamura, M. Kinoshita, P. Rey, J. Cerujeda, and J. Veciana, Phys. Rev. B **55**, 8398 (1997).
[18] J.H. Van Vleck, Phys. Rev. **78**, 266 (1950).
[19] C. Kittel, Phys. Rev. **73**, 155 (1948).